

Crystalline Behavior and Microstructure Analysis in $\text{Fe}_{73.28}\text{Si}_{13.43}\text{B}_{8.72}\text{Cu}_{0.94}\text{Nb}_{3.63}$ Alloy

Young Hwa Oh, Yoon Bae Kim¹, Hyun Kwang Seok¹, Young-Woon Kim*

School of Materials Science and Engineering, Research Institute of Advanced Materials, Seoul National University, Seoul 08826, Korea

¹*Center for Bio Materials, Korea Institute of Science and Technology, Seoul 02792, Korea*

*Correspondence to:
Kim YW,
Tel: +82-2-880-7977
Fax: +82-2-880-7977
E-mail: youngwk@snu.ac.kr

Received March 13, 2017

Revised March 27, 2017

Accepted March 28, 2017

The microstructure, the crystallization behavior, and magnetic properties of FeSi-based soft magnetic alloys (FINEMET) were investigated using transmission electron microscopy, X-ray diffraction, and coercive force measurements. The amorphous $\text{Fe}_{73.28}\text{Si}_{13.43}\text{B}_{8.72}\text{Cu}_{0.94}\text{Nb}_{3.63}$ alloys particles, prepared in 10^{-4} torr by gas atomization process, were heat treated at 530°C, 600°C, and 670°C for 1 hour in a vacuum of 10^{-2} torr. Nanocrystalline Fe precipitation was first formed followed by the grain growth. Phase formation and crystallite sizes was compared linked to its magnetic behavior, which showed that excellent soft magnetic property can directly be correlated with its microstructure.

Key Words: Coercive force, Differential thermal analysis, EELS, Selected area diffraction patterns, Niobium

INTRODUCTION

The crystallization behavior of FeSiB-based soft magnetic alloys was extensively investigated over the last decade. Yoshizawa et al. (1988) reported that soft magnetic properties were observed with the optimum heat-treatment condition of 550°C for 1 hour in the 1 at% Cu and 3 at% Nb added Fe-Si-B alloy, which is known as FINEMET (Hono et al., 1991, 1992). The microstructure of FIMENET consists of ultrafine grains of bcc phase with a few nanometers in diameter, which is believed to contribute to the excellent soft magnetic properties (Yoshizawa & Yamauchi, 1990). It was known that the magnetic behavior of these materials was strongly influenced by the formation of crystalline phases and its microstructure. In order to correlate the microstructural transition and the magnetic properties, the early stage behavior of the primary crystallization has been studied over the years, using techniques that include atom probe field ion microscopy, high-resolution electron microscopy (Yoshizawa & Yamauchi, 1991), extended X-ray absorption fine structure analysis (Ayers et al., 1998). In order to refine the microstructure,

niobium was added and the effect on the microstructural refinement has also been studied (Lecaude & Perron, 1997). Crystallization behavior at high temperature, called as the 2nd crystallization, can be a critical factor on the magnetic properties because of the high driving force at elevated temperature delivering large crystallites. In this paper, we investigated and report the microstructural transition and the physical properties of amorphous $\text{Fe}_{73.28}\text{Si}_{13.43}\text{B}_{8.72}\text{Cu}_{0.94}\text{Nb}_{3.63}$ alloy was investigated using transmission electron microscopy (TEM) and coercive force measurement, with heat treatments to achieve maximum performance of magnetic properties.

MATERIALS AND METHODS

The specimen had basic composition of 13.43% Si, 8.72% B, 0.94% Cu, and 3.63% Nb, with balanced Fe in atomic%. Molten alloy was atomized to make amorphous powders of 75~100 μm in diameter in vacuum of 10^{-2} Pascal. The atomized alloy specimens were annealed at 530°C, 600°C, and 670°C for 1 hour under 1 Pascal pressure. Coercive force was measured from each sample after each heat-treatment

temperature.

Crystalline behavior and phase analysis of the alloys were carried out using differential thermal analysis (DTA) and X-ray diffraction (XRD) using CuK_α radiation. Scanning transmission electron microscopy (STEM), operated at 200 kV, was used to analyze the morphological changes, structural and chemical information of the alloys. Electron energy loss spectroscopy and energy dispersive spectroscopy in STEM were adopted to obtain 2-dimensional distribution of the light and heavy elements in amorphous and crystalline region of the alloys, respectively. Cross-sectional TEM specimens were prepared using focused ion beam.

RESULTS AND DISCUSSION

Fig. 1 shows the crystalline characteristic of the amorphous $\text{Fe}_{73.28}\text{Si}_{13.43}\text{B}_{8.72}\text{Cu}_{0.94}\text{Nb}_{3.63}$ alloy with heat-treatment temperatures obtained from DTA at a heating rate of $20^\circ\text{C}/$

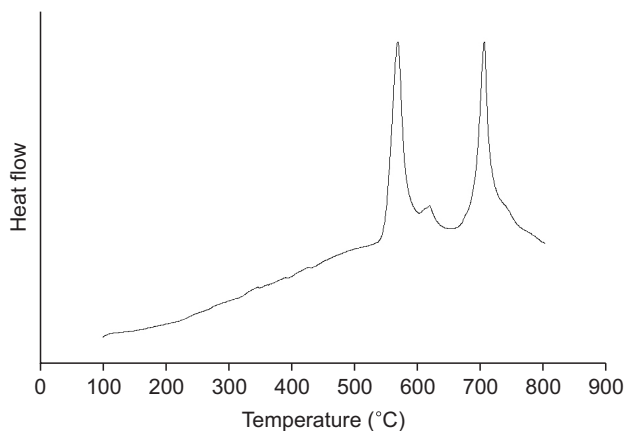


Fig. 1. Differential thermal analysis thermograms of the $\text{Fe}_{73.28}\text{Si}_{13.43}\text{B}_{8.72}\text{Cu}_{0.94}\text{Nb}_{3.63}$ alloy at heating rate of $20^\circ\text{C}/\text{min}$.

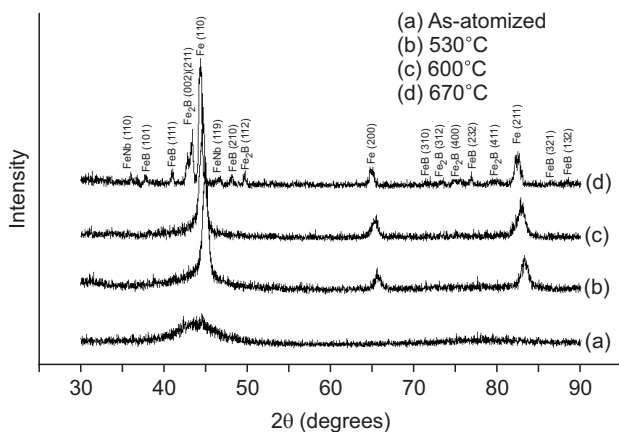


Fig. 2. X-ray diffraction patterns of the as-atomized phases (a), annealed for 1 hour at 530°C (b), annealed for 1 hour at 600°C (c), and annealed for 1 hour at 670°C (d) of the $\text{Fe}_{73.28}\text{Si}_{13.43}\text{B}_{8.72}\text{Cu}_{0.94}\text{Nb}_{3.63}$ alloy.

min. The thermogram revealed two distinct exothermic peaks, which meant that the amorphous alloy went through two crystallization steps, at 543°C and 675°C . Fig. 2 shows XRD spectrum obtained from as-atomized, annealed at 530°C , 600°C , and 670°C . First crystalline phases of the exothermic peak in the DTA was from the formation of BCC Fe, which was clearly identified from the XRD peak in Fig. 2(b) and 2(c). The second phases appeared in DTA curve were from the formation of FeB, Fe₂B, and FeNb intermetallic compound as identified in Fig. 2(d). As crystallization proceeds, the peak position of bcc Fe phases shifted due to the formation of Fe-based compounds as will be discussed in the later section.

Fig. 3 shows changes of the coercive force (H_c) with heat

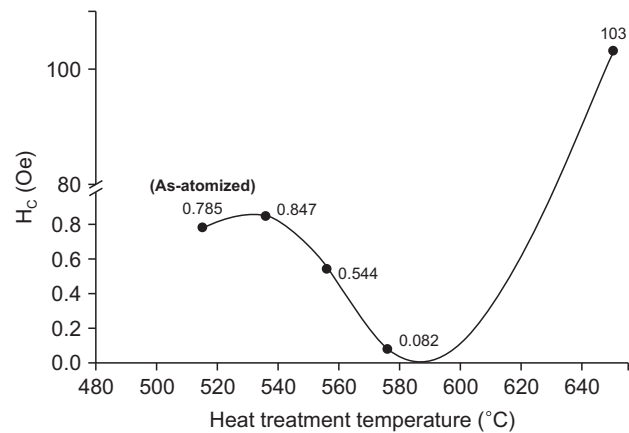


Fig. 3. Coercive force (H_c) as a function of heat-treatment temperature for the $\text{Fe}_{73.28}\text{Si}_{13.43}\text{B}_{8.72}\text{Cu}_{0.94}\text{Nb}_{3.63}$ alloy.

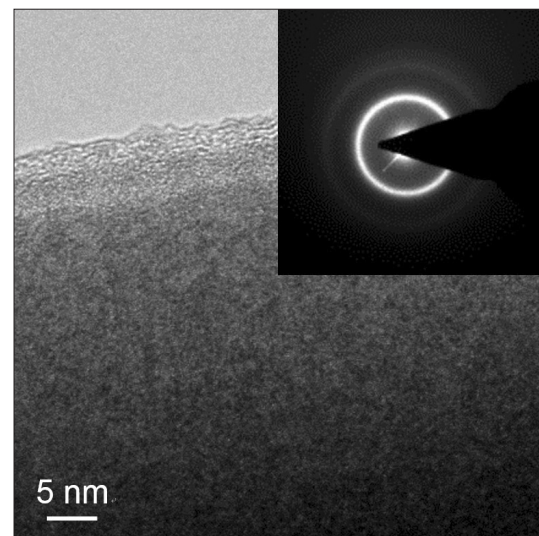


Fig. 4. Transmission electron microscopy photographs and energy dispersive spectroscopy spectrum of as-atomized $\text{Fe}_{73.28}\text{Si}_{13.43}\text{B}_{8.72}\text{Cu}_{0.94}\text{Nb}_{3.63}$ alloy. Halo ring pattern, characteristic diffraction pattern from amorphous phase, is observed and shown in the inset.

treatments. As the treatment temperature increased, H_C was reduced to 0.082 Oe at 575°C, close to the first peak temperature of DTA curve, 570°C, which reveal the start temperature of crystallization, ~535°C. After the minimum H_C point, a rapid increase of H_C was observed with the heat-treatment temperature above 600°C. Microstructural investigations were carried out to correlate the microstructure and the soft magnetic properties to identify the major microstructure for the enhancement of magnetic properties. Fig. 4 shows the microstructure of the as-atomized with the selected area diffraction patterns (SADP) in the inset. No distinct feature or segregation of the alloying elements (Si, B, Nb, Cu) was observed in the powder as can be seen. SAD shows faint, diffuse higher order index rings, which might be due to the crystal size effect broadening peaks in SAD and XRD.

The sample was heat-treated at close to the first crystallization temperature in DSC curve, at 576°C, and the microstructure and SADP are shown in Fig. 5. Fine crystalline grains of about 10~20 nm in diameter were formed throughout the powder, which was believed to play a major role in achieving the excellent soft magnetic properties. Nanocrystalline BCC phase, embedded in the amorphous phases, were identified as Fe crystals from XRD, SADP and nano-beam diffraction

method. These nano-scale Fe phases might influence magnetic properties, such as magnetostriction, coercive force, and magnetic anisotropy, as reported earlier (Yoshizawa et al., 1988).

As the heat-treatment temperature is further increased, the number of the bcc Fe crystals increased and copper crystalline grains started to appear. Fig. 6 shows the brightfield image and the elemental mapping of the microstructure which reveals distribution of copper-rich crystals in $\text{Fe}_{73.28}\text{Si}_{13.43}\text{B}_{8.72}\text{Cu}_{0.94}\text{Nb}_{3.63}$ alloys annealed at 600°C. No clustering of other elements, like niobium, was observed. Niobium was known to have limited insolubility in iron matrix, which suppresses the growth of pre-formed nuclei. Formation of Cu-rich crystallites at 600°C heat-treatment provided an increased number density of nucleation sites for the bcc crystalline phase, with the additional effect of Nb in the amorphous matrix. Combined effect of Cu-rich phase and Nb, equivalent to the enhancement of nucleation sites and suppression of the nuclei growth, respectively, results in the formation of the ultrafine grain structures. These ultrafine grains give relatively low coercive force, eventually leading to good soft magnetic properties (Herzer, 1989, 1990, 1995).

At 670°C grain growth occurred leading to coarser grains as shown in Fig. 7. Number density of copper-rich grains

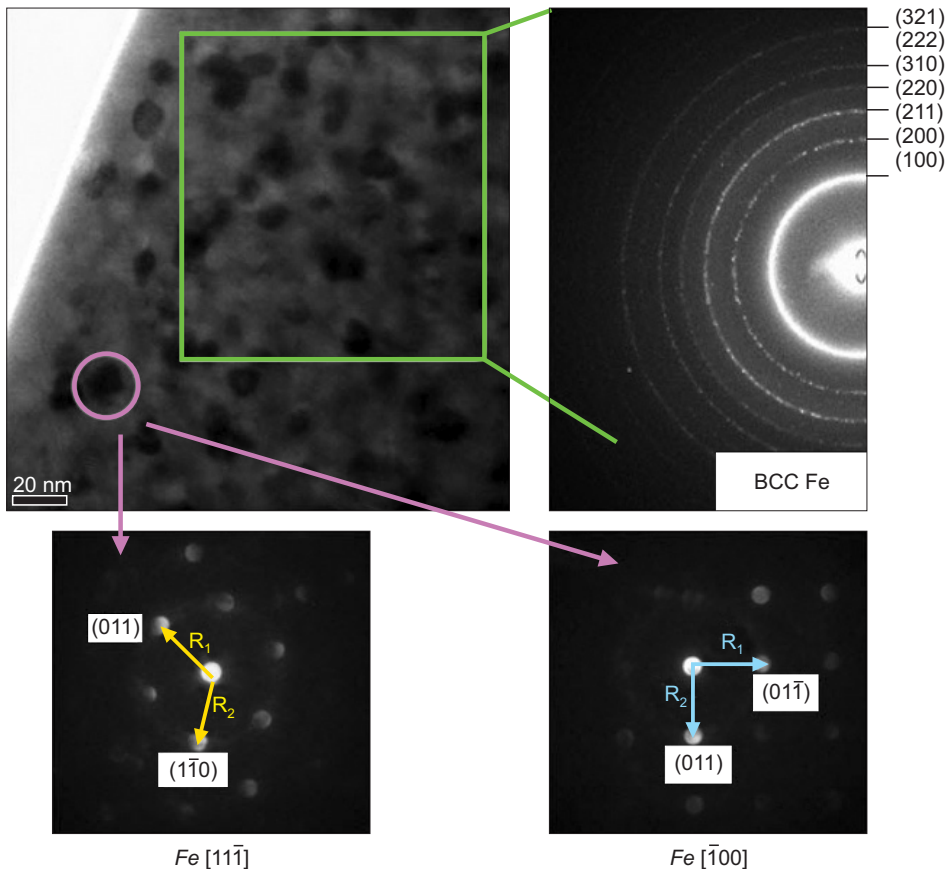


Fig. 5. Microstructure and nano-beam diffraction of the alloy heat treated at 576°C.

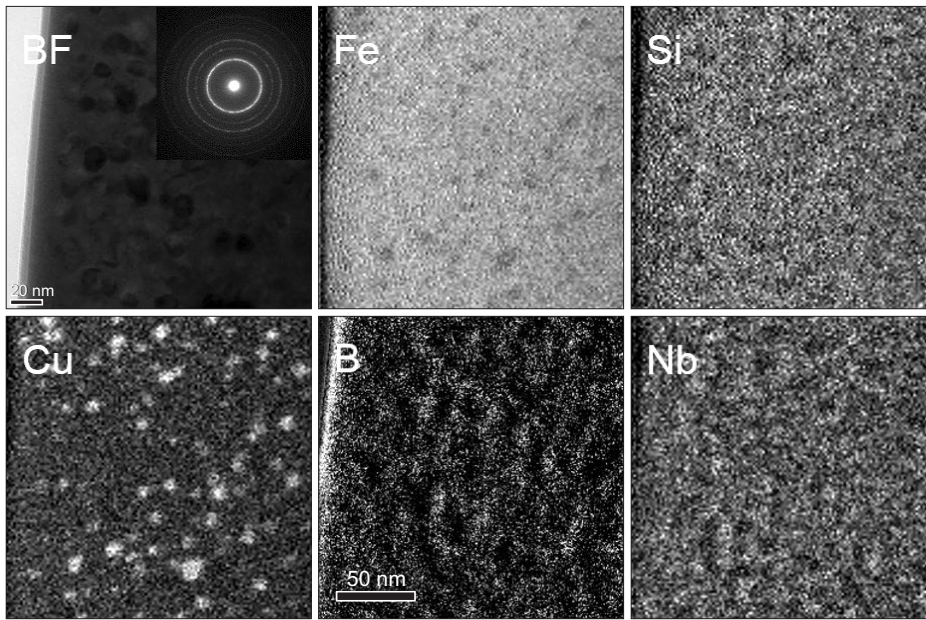


Fig. 6. Transmission electron microscopy photographs of $\text{Fe}_{73.28}\text{Si}_{13.43}\text{B}_{8.72}\text{Cu}_{0.94}\text{Nb}_{3.63}$ alloy annealed for 1 hour at 600°C.

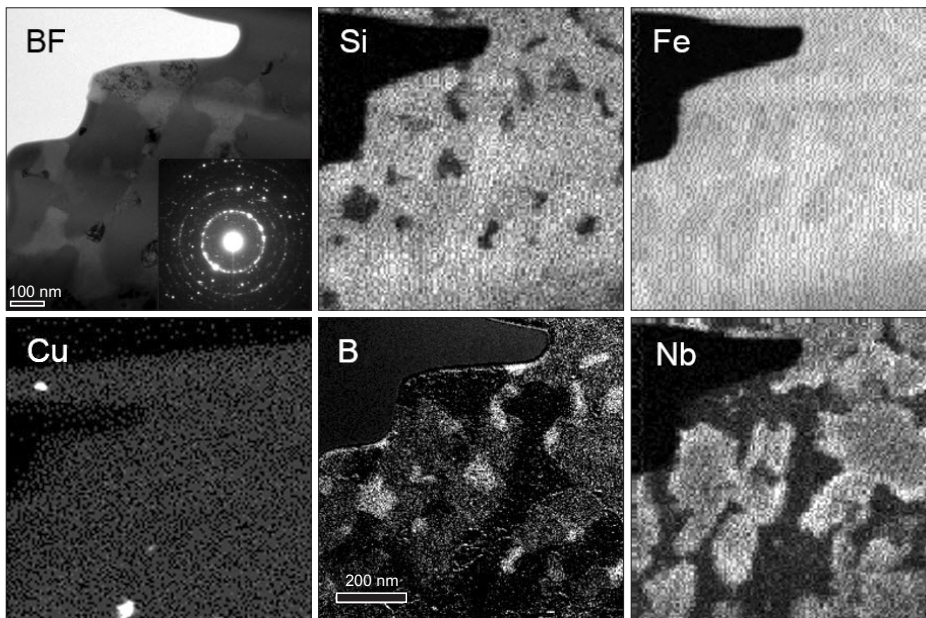


Fig. 7. Transmission electron microscopy photographs of $\text{Fe}_{73.28}\text{Si}_{13.43}\text{B}_{8.72}\text{Cu}_{0.94}\text{Nb}_{3.63}$ alloy annealed for 1 hour at 670°C.

noticeable decreased and it is clearly visible that the B-rich and N-rich phase got separated. It clearly reveals that the separation of B-rich, Si-rich, and Si-rich phases. B-rich and Si-rich phase formed compensating structure each other while niobium showed intermixing with silicon but not with boron. Degradation of soft magnetic properties was observed above 600°C of heat treatment, which commonly reveals the reduction of copper-rich phase and the grain growth. It is believed that the grain growth and the elemental localization were the main causes of the increase in coercive force.

CONCLUSIONS

Microstructural evolution and the magnetic properties were correlated in the rapidly solidified $\text{Fe}_{73.28}\text{Si}_{13.43}\text{B}_{8.72}\text{Cu}_{0.94}\text{Nb}_{3.63}$ alloy with different heat treatment temperatures. Fig. 8 shows the schematic view of the microstructural evolution. In the as-atomized stage, the alloy is a structurally and chemically homogenous amorphous phase. At the optimum stage of magnetic properties, which was obtained by heat treatment at ~580°C, Cu rich clusters were formed with a few nanometer in diameter, which contribute to the maximum

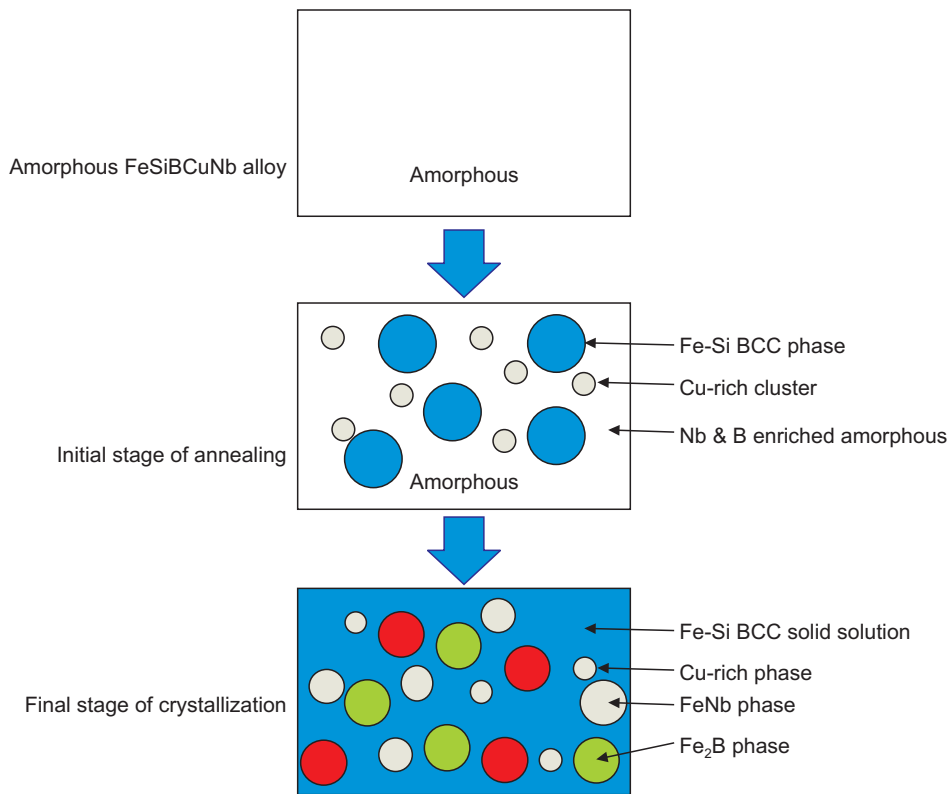


Fig. 8. Schematic diagrams of the evolution of the microstructure of $\text{Fe}_{73.28}\text{Si}_{13.43}\text{B}_{8.72}\text{Cu}_{0.94}\text{Nb}_{3.63}$ alloy with the heat-treatment temperature.

performance of magnetic properties. At temperature above 675°C , phase separation of B-rich, Nb-rich, and Si rich phases were observed and the number density of copper-rich phase reduced significantly.

CONFLICT OF INTEREST

No potential conflict of interest relevant to this article was reported.

ACKNOWLEDGMENTS

Financial support from “the Nano Material Technology Development Program (Green Nano Technology Development Program) through the National Research Foundation of Korea funded by the Ministry of Science, ICT & Future Planning (2011-0019984)” is gratefully acknowledged.

REFERENCES

- Ayers J D, Harris V G, Sprague J A, Elam W T, and Jones H N (1998) On the formation of nanocrystals in the soft magnetic alloy $\text{Fe}_{73.5}\text{Nb}_3\text{Cu}_1\text{Si}_{13.5}\text{B}_9$. *Acta Materialia* **46**, 1861-1874.
- Herzer G (1989) Grain structure and magnetism of nanocrystalline ferromagnets. *IEEE Trans. Magn.* **25**, 3327-3329.
- Herzer G (1990) Grain size dependence of coercivity and permeability in nanocrystalline ferromagnets. *IEEE Trans. Magn.* **26**, 1397-1402.
- Herzer G (1995) Soft magnetic nanocrystalline materials. *Scripta Metallurgica et Materialia* **33**, 1741-1756.
- Hono K, Hiraga Q, Wang A, Inoue T, and Sakurai T (1992) The microstructure evolution of a $\text{Fe}_{73.5}\text{Si}_{13.5}\text{B}_9\text{Nb}_3\text{Cu}_1$ nanocrystalline soft magnetic material. *Acta Metallurgica et Materialia* **40**, 2137-2147.
- Hono K, Inoue A, and Sakurai T (1991) Atom probe analysis of $\text{Fe}_{73.5}\text{Si}_{13.5}\text{B}_9\text{Nb}_3\text{Cu}_1$ nanocrystalline soft. *Appl. Phys. Lett.* **58**, 2180.
- Lecaude N and Perron J C (1997) Nanocrystallization mechanisms in Finemet-type alloys from calorimetric studies. *Mater. Sci. Eng.: A* **226-228**, 581-585.
- Yoshizawa Y, Oguma S, and Yamauchi K (1988) New Fe-based soft magnetic alloys composed of ultrafine grain structure. *J. Appl. Phys.* **64**, 6044.
- Yoshizawa Y and Yamauchi K (1990) Fe-Based soft magnetic alloys composed of ultrafine grain structure. *Mater. Trans. JIM* **31**, 307-314.
- Yoshizawa Y and Yamauchi K (1991) Magnetic properties of Fe-Cu-M-Si-B (M = Cr, V, Mo, Nb, Ta, W) alloys. *Mater. Sci. Eng.: A* **133**, 176-179.